Development 127, 3031-3044 (2000)
Printed in Great Britain © The Company of Biologists Limited 2000
DEV3208



# An orthologue of the *kit*-related gene *fms* is required for development of neural crest-derived xanthophores and a subpopulation of adult melanocytes in the zebrafish, *Danio rerio*

**David M. Parichy[1,2,*], David G. Ransom[3], Barry Paw[3], Leonard I. Zon[3] and Stephen L. Johnson[1]**

[1]Department of Genetics, Washington University Medical School, St Louis, MO 63110, USA
[2]Section of Integrative Biology and Institute for Cellular and Molecular Biology, University of Texas at Austin, Austin TX 78712, USA
[3]Department of Medicine, Childrens' Hospital of Boston, Howard Hughes Medical Institute, 300 Longwood Avenue, Enders 7, Boston MA 02115, USA
*Author for correspondence (e-mail: dparichy@genetics.wustl.edu)

*Accepted 5 May; published on WWW 22 June 2000*

## SUMMARY

**Developmental mechanisms underlying traits expressed in larval and adult vertebrates remain largely unknown. Pigment patterns of fishes provide an opportunity to identify genes and cell behaviors required for postembryonic morphogenesis and differentiation. In the zebrafish, *Danio rerio*, pigment patterns reflect the spatial arrangements of three classes of neural crest-derived pigment cells: black melanocytes, yellow xanthophores and silver iridophores. We show that the *D. rerio* pigment pattern mutant *panther* ablates xanthophores in embryos and adults and has defects in the development of the adult pattern of melanocyte stripes. We find that *panther* corresponds to an orthologue of the c-*fms* gene, which encodes a type III receptor tyrosine kinase and is the closest known homologue of the previously identified pigment pattern gene, *kit*. In mouse, *fms* is essential for the development of macrophage and osteoclast lineages and has not been implicated in neural crest or pigment cell development. In contrast, our analyses demonstrate that *fms* is expressed and required by *D. rerio* xanthophore precursors and that *fms* promotes the normal patterning of melanocyte death and migration during adult stripe formation. Finally, we show that *fms* is required for the appearance of a late developing, *kit*-independent subpopulation of adult melanocytes. These findings reveal an unexpected role for *fms* in pigment pattern development and demonstrate that parallel neural crest-derived pigment cell populations depend on the activities of two essentially paralogous genes, *kit* and *fms*.**

Key words: Melanocyte, Xanthophore, Zebrafish, Pigment pattern, *fms*

## INTRODUCTION

Recent years have seen dramatic advances in our understanding of the developmental genetic bases for the patterning of embryonic axes, tissues and organ rudiments. In contrast, we know relatively little about mechanisms underlying the expression of traits during later stages of development and in adults (Tata, 1993). Nevertheless, identifying the genes and cell behaviors underlying trait expression is an essential step in understanding the origins of naturally occurring trait variation and the evolution of form (Atchley and Hall, 1991; Phillips, 1999). One ecologically important trait that is particularly amenable to analysis is the externally visible pigment pattern of fishes in the genus *Danio*, which includes the zebrafish *D. rerio*.

Pigment cells in *Danio* and other vertebrates are derived from neural crest cells that arise along the dorsal neural tube then disperse along stereotypical pathways throughout the embryo (Hörstadius, 1950; Erickson and Perris, 1993; Hall, 1999; Groves and Bronner-Fraser, 1999). In addition to pigment patterns, neural crest cells contribute to a host of other tissues and organ systems in vertebrates, including bones of the craniofacial skeleton, teeth, neurons and glia of the peripheral nervous system, endocardial cushion cells and endocrine glands. Indeed, Gans and Northcutt (1983) have argued that much of vertebrate morphology and its evolution can be understood in terms of the patterning of neural crest cells and their derivatives, and how these patterning mechanisms have changed phylogenetically. Elucidating the mechanisms by which the final form of larval and adult pigment patterns arise may thus shed light on more general mechanisms of trait variation and evolution in vertebrates.

In danios and many other ectothermic vertebrates, pigment patterns result from the spatial arrangements and coloration of three major classes of neural crest-derived pigment cells: black melanocytes (or melanophores), yellow xanthophores and silver iridophores (Bagnara, 1998; Reedy et al., 1998). In *D. rerio*, these different classes of pigment cell combine to

generate different pigment patterns during different phases of the life cycle (Kirschbaum, 1975; Johnson et al., 1995b). In larvae, a relatively simple pattern is evident by hatching (approx. 2.5 days; Fig. 1A). This 'early larval' pigment pattern consists of several stripes of melanocytes and iridophores, as well as xanthophores that are widely distributed over the flank, giving an overall yellow cast to the body. This pattern persists until approx. 14 days, at which time a metamorphosis begins that ultimately results in the formation of the striped pigment pattern of the adult (Fig. 1C). Between 14 and 21 days, melanocytes increase in number and become visible dispersed throughout the skin in regions not previously occupied by these cells. Subsequently, between 21 and 28 days, melanocyte numbers increase more sharply and an adult stripe pattern begins to emerge. This pattern comprises two melanocyte stripes by 28 days, but additional stripes form as the fish grow. Dark stripes consist of melanocytes and iridophores, whereas light 'interstripe' regions consist of xanthophores and iridophores (Fig. 2A). Finally, in addition to stripes that are found deep within the dermis adjacent to the myotomes (Hawkes, 1974), more superficial melanocytes and xanthophores cover the dorsal scales, and together give a dark cast to the dorsum of the fish.

The mechanisms of adult stripe development remain largely unknown in *D. rerio*. Nevertheless, several mutants have started to provide insights into the genes and cell populations that are involved in pigment pattern metamorphosis in this species. A previous analysis (Johnson et al., 1995b) identified roles for three genes that are required for the development of adult stripes: *sparse*, *rose* and *leopard*. *sparse* mutant larvae have fewer melanocytes than wild type at 3 days. These cells then die, and the fish completely lack melanocytes until approx. 21 days, when a new population differentiates and contributes to an adult pigment pattern with one-half the wild-type complement of stripe melanocytes. In contrast, *rose* and *leopard* mutants each exhibit normal pigment patterns through 21 days, but melanocyte numbers increase less rapidly than wild type between 21 and 28 days, again resulting in one-half the wild-type complement of stripe melanocytes. These findings suggested that *sparse* on one hand, and *rose* and *leopard* on the other, identify genes required for the development of distinct classes of melanocytes in the adult pigment pattern: an early developing adult population dependent on *sparse*; and a later developing adult population dependent on *rose* and *leopard*. In support of this model, virtually all body stripe melanocytes are ablated in fish homozygous for both *sparse* and *rose* mutations, or *sparse* and *leopard* mutations, whereas no additional melanocyte deficit is found in fish homozygous for *rose* and *leopard* mutations, as compared to either single mutant alone. Thus, the pigment pattern of adult *D. rerio* depends on contributions from temporally and genetically distinct populations of melanocytes, dependent on the activities of either *sparse* (early appearing melanocytes), or *rose* and *leopard* (later appearing melanocytes). More recently, we showed that *sparse* is a zebrafish orthologue of *kit*, which encodes a type III receptor tyrosine kinase that has long been studied for its role in pigment pattern development in amniotes (Parichy et al., 1999). What additional genes contribute to the morphogenesis and differentiation of these melanocyte populations, and other pigment cell classes, remain largely unknown.

Here, we identify another gene required for stripe development in *D. rerio*. We show that the pigment pattern mutant *panther* corresponds to an orthologue of c-*fms*, which is the closest known homologue of the previously identified pigment pattern gene *kit*. We find that *fms* is required for the morphogenesis of embryonic xanthophore precursors and the development of adult xanthophores. We also demonstrate roles for *fms* during adult stripe development. *fms* promotes the normal patterning of cell death and migration among early larval melanocytes and *kit*-dependent (*rose*-independent) stripe melanocytes. *fms* is also essential for the differentiation of late appearing, *rose*-dependent (*kit*-independent) stripe melanocytes. These findings indicate that two essentially paralogous genes (*fms*, *kit*) promote the morphogenesis and differentiation of parallel pigment cell populations in *D. rerio*.

## MATERIALS AND METHODS

### Fish rearing, mutant alleles, genetic mapping, cloning and molecular analysis

Rearing of *D. rerio* followed Westerfield (1993). All mutant *panther* alleles analyzed are recessive and exhibit pigment patterns that are indistinguishable from one another. *panther*$^{j4e1}$ was induced by the point mutagen ethyl nitrosourea (ENU) in the AB genetic background (Johnson and Zon, 1999). *panther*$^{j4blue}$ was identified as an allele of *panther* by complementation testing of 'blue' variety *D. rerio* obtained from the pet trade. Finally, *panther*$^{j4e2}$ was induced by ENU in the inbred C32 genetic background.

To map *panther*, we crossed *panther*$^{j4e1}$ (maintained in the C32 background) to the inbred wild-type strain SJD to produce highly polymorphic progeny segregating alleles of C32/AB and SJD strains. To rapidly focus our mapping efforts, we used half-tetrad centromere linkage analysis (Johnson et al., 1995a) to exclude chromosomes from consideration. We produced gynogenetic offspring from polymorphic *panther*$^{j4e1}$/+ females, reared these to maturity, then scored them for

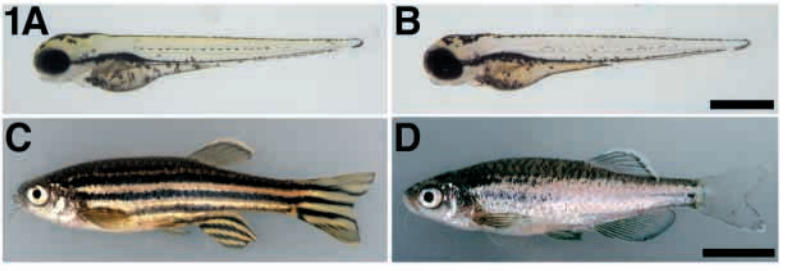


**Fig. 1.** Larval and adult pigment patterns of *D. rerio*. (A,C) Wild-type and (B,D) *panther* mutants. (A) Wild-type larvae (3 days) have melanocyte and iridophore stripes, and dispersed xanthophores create an overall yellow cast to flank. (B) *panther* mutant larvae have normal melanocyte patterning, and total numbers of melanocytes do not differ significantly from wild type at 60 hours (mean±s.d., wild type: 313±44.4, $n$=6; *panther*: 279±17.5, $n$=6; $t_{10}$=1.76, $P$=0.1); iridophores are also present in apparently normal numbers. In contrast, *panther* mutant larvae lack the yellow cast of wild-type larvae, indicating a defect in xanthophore development. (C) Wild-type adults have a pattern of dark horizontal stripes with intervening interstripe regions. A dark cast to the dorsal flank is due to scale-associated melanocytes. (D) *panther* mutant adults have poorly formed stripes anteriorly and lack stripes posteriorly. Scale bars: (A,B) 600 μm; (C,D) 1 cm.

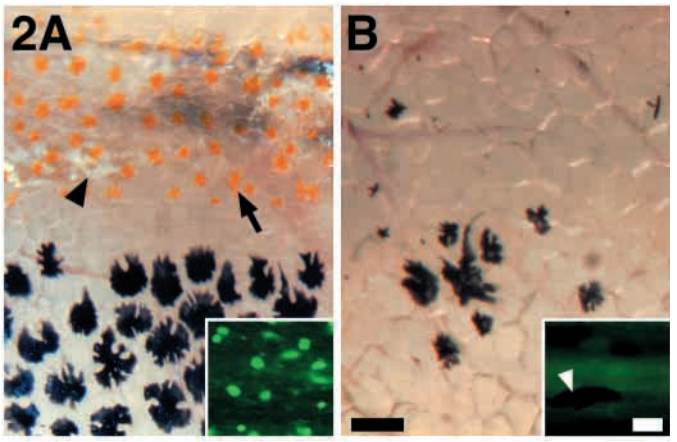


**Fig. 2.** Xanthophores are present in wild-type (A) but not *panther* mutant (B) adults (stages in Fig. 1C,D). (A) In wild-type adults, light stripes include orange xanthophores (arrow) whereas dark stripes include black melanocytes. With transmitted illumination in this image, most iridophores (arrowhead) are not visible. Inset: under ultraviolet illumination, pteridine pigments contained within xanthophores are liberated from their protein carriers resulting in a green autofluorescence that can reveal lightly pigmented xanthophores not otherwise visible (Epperlein and Löfberg, 1990). Shown here are autofluorescing xanthophores in the caudal fin of a wild-type adult. (B) In a similar region of a *panther* mutant adult, fewer melanocytes are present and xanthophores are completely absent. Iridophores are widely distributed over the flank and do not exhibit an apparent defect in comparison to wild type. Inset: only background fluorescence is visible in the caudal fin of a *panther* mutant adult, indicating an absence of pteridine-containing xanthophores. A melanocyte is indicated with an arrowhead. Scale bars: (A,B) 100 μm; (insets) 30 μm.

phenotype and isolated genomic DNA by standard procedures. We then assessed linkage to centromere markers for each of the 25 *D. rerio* chromosomes: a complete absence of SJD alleles among 8 gynogenetic *panther* adults suggested the presence of *panther* on Linkage Group (LG) 14. Subsequently, we mapped *panther* more precisely with backcross families segregating *panther*$^{j4e1}$. We cloned a partial *D. rerio fms* cDNA using degenerate reverse transcriptase PCR from a kidney cDNA library, then cloned a full-length cDNA by rapid amplification of cDNA ends (primer sequences available on request). To map *panther*$^{j4e1}$ relative to *fms* (GenBank accession #AF240639; see Results), we designed primers (forward: AGGTGAGCGAAGGAGACGATG; reverse: GTATTGGCCGATCTCCTCGAAG) to amplify a polymorphism within predicted intron 6 of the *fms* gene. Finally, to test *fms* as a candidate for *panther*, we designed primers to amplify overlapping fragments of *fms* cDNAs derived by RT-PCR, and sequenced the PCR products directly to avoid cloning artefacts. We used BigDye dye terminator chemistry (Perkin Elmer) on an ABI-377 automated sequencer and sequenced forward and reverse directions for 2-5 individuals of each genetic background. For *panther*$^{j4e1}$ and *panther*$^{j4e2}$, we compared sequences to those for ancestral chromosomes in AB and C32 backgrounds, respectively. Phylogenetic analyses were performed with PAUP 4.0.0d55 (Swofford, 1999) after aligning sequences with the Pileup program of the GCG software package, and used parsimony and heuristic searching with 1000 bootstrap replications. Nucleotide and protein sequences also were compared against existing databases by BLAST, and predicted protein domains were assessed by comparison with the Pfam database (http://pfam.wustl.edu).

### In situ hybridization

Methods for riboprobe preparation and in situ hybridization have been described (Jowett and Yan, 1996), and employed digoxigenin- and fluorescein-labeled riboprobes, alkaline phosphatase-conjugated anti-digoxigenin or anti-fluorescein Fab fragments, and NBT/BCIP (Roche, Indianapolis, IN) or FastRed (Sigma, St. Louis, MO) substrates. Hybridizations were carried out for 12-24 hours at 68°C or 70°C, followed by stringency washes at the same temperatures. Larvae >5 days were cut transversely after fixation to facilitate penetration of reagents. For *kit* (Parichy et al., 1999) and *fms*, we used full-length cDNAs (approx. 3 kb) as templates for riboprobe generation. We cloned a 540 bp fragment of *D. rerio xdh* for riboprobe synthesis (this gene is also identified as *D. rerio* EST fc18g02; accession numbers: AI657925, AI641077), and used *D. rerio* ESTs to generate riboprobes for *gch* (fa05h05; AA494989, AA494990) and *cathepsin-K* (fa95f03; AI331947, AI330487). cDNAs for *mitf* (Lister et al., 1999) and *dct* (Kelsh and Eisen, 1999) were provided by D. Raible and R. Kelsh, respectively.

### Analyses of melanocyte behaviors and distributions

To identify melanocyte behaviors that underlie the adult *panther* mutant phenotype, we followed individual melanocytes in image series of wild-type and *panther* mutant larvae ($n$=4 per genotype). Larvae were imaged at 32× using a Spot II digital imaging system (set to capture a high-speed monochrome image) interfaced to an Olympus SZX12 zoom stereomicroscope and Macintosh computer. Images were taken every 24 hours for 12 days, beginning on day 18 of development. Larvae were anesthetized long enough to record an image, then were revived and maintained individually (14 hours L:10 hours D light cycle, 2 feedings per day). All larvae developed normal wild-type or *panther* mutant adult pigment patterns.

We followed individual melanocytes by comparing melanocyte positions at each of 4-5 body regions along the anteroposterior axis. To facilitate tracking cells and analyzing different morphogenetic behaviors, we labeled individual melanocytes in each body region on day 18 (cells A-M), day 24 (cells N-R), and day 30 (cells S-Z) using Adobe Photoshop (see below). We then followed these cells forwards and backwards in the image series. Identification of different populations of cells at different times allowed us to test whether cells at the beginning of the series died later in the series, and whether cells at the end of the series were present at the beginning, or had differentiated during the time of imaging. We were able to continuously re-identify >90% of labeled melanocytes across all time points, and death of cells could be inferred by the unambiguous disappearance of a cell from one image to the next (see below). To test for movements of melanocytes, we first determined the relative dorsal-to-ventral position of each cell on the flank; a position of 0.0<0.5 is dorsal, 0.5<1.0 is ventral, and 0.5 represents the dorsoventral midpoint of the flank and the approximate position of the developing interstripe region. To assess whether cells moved dorsally or ventrally during the image series, we subtracted the dorsoventral position of each melanocyte when first identified from its position when last visible. This provided an estimate of the net change in dorsoventral position for each cell, such that values >0.0 represent a net ventral movement, and values <0.0 represent a net dorsal movement. These estimates do not, however, reflect anteroposterior changes or total distances migrated. We haphazardly picked cells to label and follow, but attempted to choose melanocytes distributed widely over the flank; dorsoventral distributions of melanocytes chosen for analysis did not differ between wild-type and *panther* mutants ($t_{878}$=0.69; $P$=0.5). In total, we were able to follow 880 melanocytes in image series of wild-type and *panther* mutant larvae.

To assess changes in melanocyte numbers over time, we counted the total numbers of these cells within each of four myotomal segments distributed evenly across the anteroposterior axis of the same larvae used for imaging. Additionally, to assess differences among genotypes, we counted melanocytes in juvenile fish that had already developed an adult pigment pattern. For these latter counts, we limited our analysis to a region bordered anteriorly and posteriorly

by the base of the anal fin; we further limited this analysis to melanocytes that were not present on scales, but were present deeper in the dermis where melanocytes normally are found that contribute to adult stripes. To control for differences in size and area among individuals, we normalized melanocyte counts according to the length of the region examined, resulting in counts with units of melanocytes/mm. Other methods of normalizing melanocyte numbers (e.g., relative to total area or height of the flank) yielded identical results.

### Statistical methods

All statistical analyses were performed with JMP Statistical Software (SAS Institute, 1998). For image series, we analysed data as univariate models (considering only effects due to genotype), as well as full, multifactorial models that controlled for effects due to interindividual variation independent of genotype. Both simple and full analyses yielded equivalent results that are presented below. Complete statistical analyses for full models and results of testing all effects are available from DMP on request. We analyzed melanocyte death using multiple logistic regression (Shanubhogue and Gore, 1987): a full model tested for effects due to genotype, individual (nested within genotype), deviation of melanocytes from the midpoint of the flank, final height of the flank, and an interaction between genotype and deviation from the midpoint (testing whether the relationship between probability of death and position depended on genotype). We analyzed melanocyte movements using multiple linear regression (Sokal and Rohlf, 1981): a full model tested for effects due to genotype, individual (nested within genotype), starting melanocyte position, total growth of the flank (controlling for passive movements due to isometric growth), segment identity (controlling for effects due to anteroposterior position), and an interaction between genotype and starting position (testing whether the relationship between starting position and movement depended on genotype). We analyzed melanocyte differentiation using multiple logistic regression: a full model consisted of effects due to genotype and starting height of the flank. All models treated individuals and interactions involving individuals as random effects (Sokal and Rohlf, 1981).

## RESULTS

### *panther* corresponds to a *D. rerio* orthologue of *fms*

*panther* mutant adult *D. rerio* have poorly formed stripes anteriorly and lack stripes posteriorly (Fig. 1D). To test roles for *panther* in promoting pigment pattern development, we first identified this locus at the molecular level. We used half-tetrad centromere linkage analysis (Johnson et al., 1995a) to map *panther*$^{j4e1}$ to LG 14, and subsequently mapped *panther*$^{j4e1}$ in a 161 individual mapping panel between microsatellites z5435 and z1536 (Fig. 3A). Interestingly, we had previously mapped to this same interval an orthologue of the c-*fms* gene (*fms*; also known as *colony stimulating factor 1 receptor, Csf1r*). *fms* encodes a type III receptor tyrosine kinase and is the closest known homologue of *kit* in *D. rerio* (Fig. 3B); *fms* and *kit* are believed to have arisen by duplication of a common ancestral gene during the evolution of vertebrates (Yarden and Ullrich, 1988; Rousset et al., 1995). *fms* in amniotes has roles in the development of macrophages and bone-resorbing osteoclasts (Motoyoshi, 1998; Flanagan and Lader, 1998), and has not been implicated in neural crest or pigment pattern development. Nevertheless, the structural similarity of *fms* to *kit*, and the linkage between *fms* and *panther*$^{j4e1}$, led us to test *fms* as a candidate for *panther*.

To test the correspondence of *fms* and *panther*, we identified a length polymorphism within predicted intron 6 of *fms* [repeating GAAT and TGG motifs; wild-type (SJD) allele: 1000 bp; *panther*$^{j4e1}$ (AB) allele: 820 bp] and used this to assess segregation relative to the *panther* mutant phenotype. We identified 160 non-recombinant individuals, placing the *panther*$^{j4e1}$ mutant lesion approx. 0.6 cM from *fms* intron 6. Given the relatively large size of the *fms* gene in humans (32 kb coding region; Roberts et al., 1988), we hypothesized that *panther*$^{j4e1}$ might correspond to a lesion located within *fms* but relatively distant from intron 6. To test this possibility, we sequenced *fms* cDNAs from wild-type and *panther*$^{j4e1}$ mutant backgrounds. We identified a single, non-conservative (val→met) substitution in predicted exon 12, within the first kinase domain at a site that is otherwise invariant in all receptor

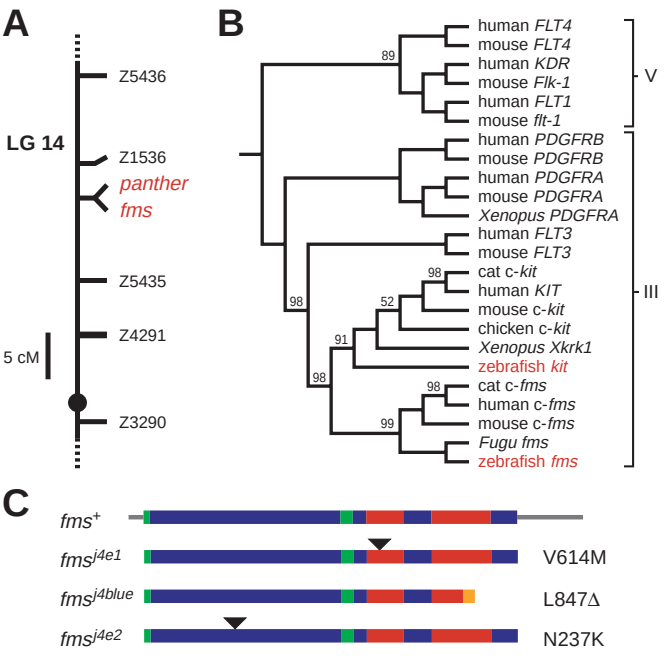


**Fig. 3.** *panther* corresponds to a *D. rerio* orthologue of *fms*. (A) Meiotic mapping found no recombinants between *panther*$^{j4e1}$ and a lesion in exon 12 of *fms*$^{j4e1}$. Microsatellite loci on LG 14 used for mapping *panther* are shown. The centromere is indicated with a circle. (B) Phylogenetic analyses for amino acids (925 informative characters) and nucleotides (not shown) demonstrates that *D. rerio fms* is the closest known homologue of *D. rerio kit*, and is orthologous to previously described *fms* genes in mammals and the pufferfish, *Fugu*. Type III and type V receptor tyrosine kinases are shown. Bootstrap support for all clades is 100% except where indicated by numbers in the cladogram. (GenBank accession numbers, top to bottom: 4503752; 293780; 3132832; 50976; 3132830; 2809068; 4505682; 53618; 189733; 200274; 214652; 406322; 50978; 913503; 4557694; 50423; 303532; 763033; 153446; 163854; 29899; 50980; 60063; 240639.) (C) Wild-type and *fms* mutant cDNAs. The wild-type *fms* cDNA open reading frame comprises 2931 bp and 977 amino acids, and includes a predicted signal sequence (green), transmembrane domain (green) and split kinase domains (red; amino acids 584-680, 752-915) all typical of this class of receptor tyrosine kinase. Untranslated regions are shown in grey. *fms* mutant cDNAs are shown with positions of corresponding substitutions indicated by arrowheads for *fms*$^{j4e1}$ and *fms*$^{j4e2}$; for *fms*$^{j4blue}$, novel amino acids resulting from a frameshift in the second kinase domain are indicated in orange.

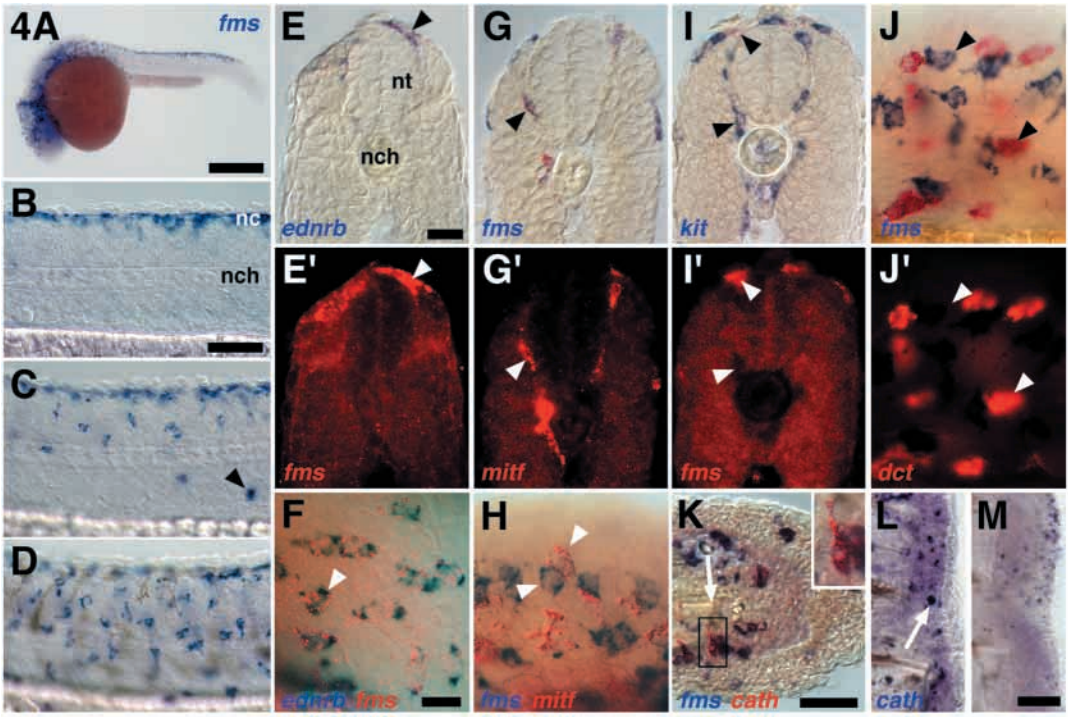


**Fig. 4.** *fms* is expressed by a subset of neural crest-derived cells as well as osteoclasts. (A-D) *fms*+ cells are present in neural crest migratory pathways during neural crest migration. (A) Whole-mount 24 hour embryo showing blue *fms*+ cells dispersing from the neural crest. (B) Lateral view of middle trunk *fms*+ cells in the premigratory neural crest (nc) in a 23 hour embryo. nch, notochord. (C) *fms*+ cells in the dorsolateral neural crest migratory pathway of a 25 hour embryo. Arrowhead indicates a *fms*+ macrophage precursor medially. (D) *fms*+ cells are interspersed with lightly pigmented melanocytes in a 28 hour embryo. (E-J) Two color in situ hybridization reveals *fms* expression by a subset of neural crest-derived cells. (E,F) Many dispersing neural crest cells (e.g., arrowhead) coexpress *ednrb* (blue) and *fms* (red). (E,E′) Corresponding bright-field and epifluorescence views of 12 μm cryosections through the trunk of a 24 hour embryos. (F) Merged bright-field and epifluoresence images of *ednrb*+ *fms*+ neural crest cells on the dorsal head of a 24 hour whole-mount embryo. (G,H) Some *fms*+ neural crest cells (blue) coexpress *mitf*+ (red). (G,G′) Corresponding views of a section through the trunk of a 24 hour embryo. (H) Merged bright-field and epifluorescence images showing developmentally more advanced neural crest cells that do not coexpress *fms* and *mitf* (arrowheads) dorsal to the midbrain-hindbrain junction of a 24 hour whole-mount embryo. (I,I′) *kit*+ neural crest cells (blue) typically do not coexpress *fms*. Cryosections through a 24 hour embryo (e.g., arrowheads). (J,J′) *fms* (blue) is not expressed by *dct*+ melanoblasts (red) and melanocytes (e.g., arrowheads). (K-M) *fms* exhibits conserved roles in osteoclastogenesis. (K) In the regenerating adult caudal fin (15 μm frontal cryosection), *cathepsin-K*+ osteoclasts (red) localize near the cut edge of lepidotrichia (arrow) and coexpress *fms* (blue; e.g., boxed cell and inset: higher magnification of the same cell). (L,M) Lateral views of whole-mount, 2 day regenerating fins. (L) In wild-type regenerates, *cathepsin-K*+ osteoclasts (arrow) are abundant. (M) In *fms* mutant regenerates, there are fewer *cathepsin-K*+ cells (although *fms* mutants do not exhibit gross regeneration defects or other skeletal anomalies). Scale bars: (A) 300 μm. (B-D) 60 μm. (E,G,I,J) 20 μm. (F,H) 20 μm. (K) 40 μm. (L,M) 80 μm.

tyrosine kinases used for our phylogenetic analysis (Fig. 3B,C). This lesion segregated with the *panther* mutant phenotype in all 161 individuals of the mapping cross, supporting the allelism of *panther* and *fms*.

To further test the correspondence of *panther* and *fms*, we sequenced *fms* cDNAs from additional *panther* backgrounds. In *panther*$^{j4blue}$, we identified a 5 nucleotide deletion near the middle of the second kinase domain, leading to 32 novel amino acids and a premature stop codon. In *panther*$^{j4e2}$, induced in a defined genetic background, we identified a non-conservative asp→arg substitution within the third immunoglobulin loop of the extracellular domain (Yarden and Ullrich, 1988; Fig. 3C). These independent *fms* lesions in three *panther* mutant alleles (two of defined genetic background) confirm the correspondence of *fms* and *panther*. Thus, we here designate the mutant and its corresponding gene, *fms*. Because all three alleles are recessive and have indistinguishable pigment patterns, all are likely to be loss of function; this inference is supported by studies associating lesions in *fms* or *kit* kinase domains with reductions in kinase activity (Reith et al., 1990, 1991, 1993), and our observation that *fms* mRNA levels are dramatically reduced in *fms* mutant embryos and larvae (data not shown). These data show that Fms, a Kit-like type III receptor tyrosine kinase, is required for pigment pattern development in *D. rerio*.

## Neural crest-derived cells and osteoclasts express *fms*

In light of the pigment pattern defect in *fms* mutants, we asked whether this gene is expressed by neural crest cells or their derivatives. In situ hybridization reveals *fms*+ cells along the mid-trunk dorsal neural tube by 18 hours (not shown), and subsequently in neural crest migratory pathways (Fig. 4A-D). To verify that these cells are neural crest-derived, we tested for coexpression of *fms* and four markers of neural crest–pigment cell lineages: the heptahelical receptor *endothelin receptor B* (*ednrb*), which is expressed by precursors of all three classes of pigment cells (D. M. P., R. N. Kelsh, S. L. J., unpublished data; Nataf et al., 1996; Shin et al., 1999); the transcription factor *microphthalmia* (*mitf*), which is expressed by melanocyte precursors (melanoblasts) but is downregulated in late differentiating melanocytes (Opdecamp et al., 1997; Lister et al., 1999); and the melanin synthesis enzyme *dopachrome tautomerase* (*dct*) and *kit*, which are expressed by melanoblasts and melanocytes (Wehrle-Haller and Weston, 1995; MacKenzie et al., 1997; Parichy et al., 1999; Kelsh and Eisen,

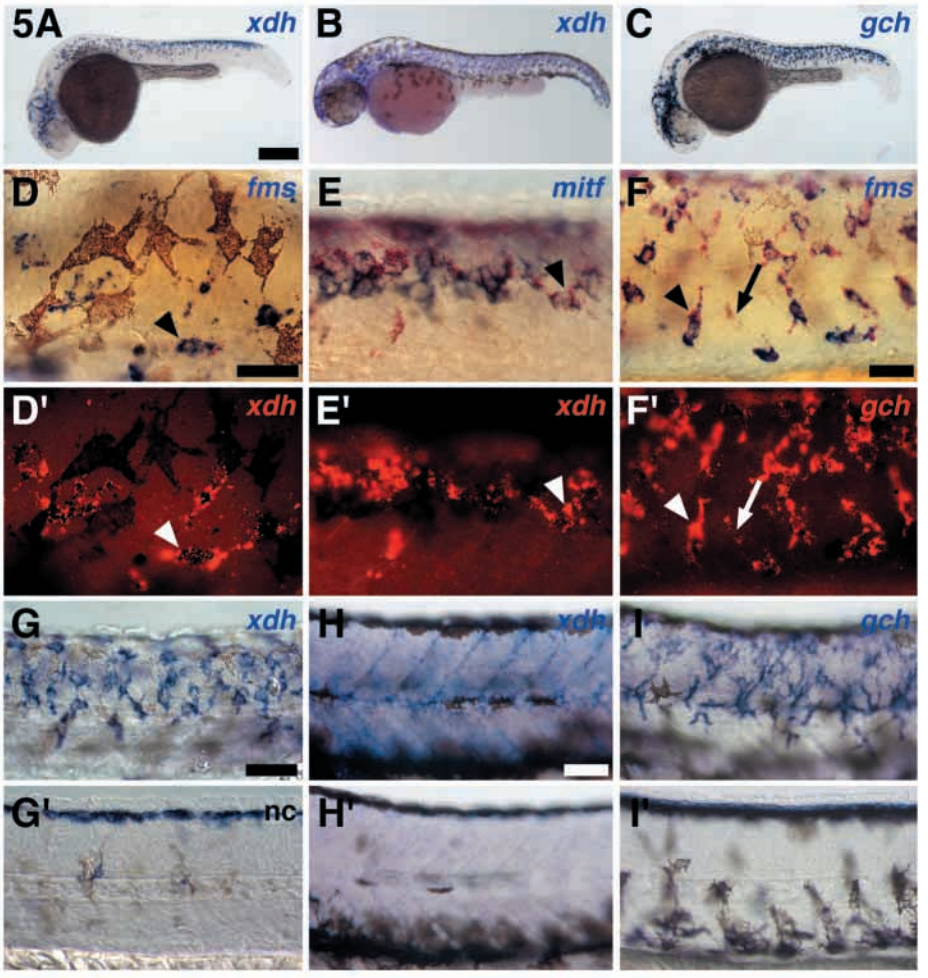


**Fig. 5.** *fms* is essential for development of embryonic xanthophores. (A-C) Dispersing neural crest cells are *xdh*+ and *gch*+. (A) *xdh*+ cells (blue) in a 26 hour embryo. (B) *xdh*+ cells cover the flank of a 36 hour embryo. (C) *gch*+ dispersing from the neural crest in a 24 hour embryo. (D,D′) Corresponding bright-field and epifluorescence views of *fms*+ (blue) cells in dorsal head of a 28 hour whole-mount embryo that coexpress *xdh* (red; e.g., arrowhead). Lightly pigmented melanocytes do not stain for either marker. (E,E′) Early migrating *mitf*+ (blue) neural crest cells coexpress *xdh* (red) as they disperse in the posterior trunk of a 24 hour whole-mount embryo. (F,F′) Unmelanized *fms*+ cells (blue) coexpress *gch* (arrowhead); lightly pigmented melanocytes also express *gch* at low levels (arrow). (G-I) Distributions of cells expressing xanthophore lineage markers differ between wild-type embryos (G,H,I) and *fms* mutant embryos (G′,H′,I′). (G,G′) At 28 hours, *xdh*+ cells are interspersed with melanocytes over the flank of wild-type embryos (G) but virtually all are confined to the premigratory neural crest (nc) in *fms* mutant embryos (G′). (H,H′) At 48 hours, *xdh*+ cells result in diffuse staining over the flank in wild type (H) but are absent in *fms* mutants (H′). (I,I′) At 32 hours, unmelanized *gch*+ cells are abundant in wild type (I) but are absent in *fms* mutants (I′). Scale bars: (A-C) 250 μm; (D,E) 30 μm; (F) 30 μm; (G,I) 50 μm; (H) 60 μm.

1999). These analyses reveal *fms* expression by *ednrb*+ cells and some *mitf*+ cells (Fig. 4E-H). In contrast, we could not detect *fms* expression by the majority of *kit*+ cells, or cells either expressing *dct* or containing melanin (Fig. 4I,J). These data demonstrate that *fms* is expressed by a subset of neural crest-derived cells, but not late stage, differentiating embryonic melanocytes.

To test whether previously described roles for *fms* in hematopoiesis and osteoclastogenesis are conserved between amniotes and teleosts, we examined *fms* expression in non-neural-crest-derived lineages. In embryos, *fms*+ cells are observed in the position of macrophage progenitors, and these cells coexpress the macrophage lineage marker *pu.1* (data not shown). Osteoclasts can be identified by the expression of the protease cathepsin-K (Roodman, 1996). In the regenerating fin, *cathepsin-K*+ presumptive osteoclasts coexpress *fms*, and *fms* mutant regenerates have fewer of these cells than wild type (mean±s.d. cells per fin in wild type: 44.1±14.98, $n$=10; *fms* mutants: 1.7±2.73, $n$=6; $t_{14}$=6.78, $P$<0.0001; Fig. 4K-M). Thus, *fms* is expressed in non-melanogenic neural crest-derived cells and has phylogenetically conserved expression in macrophage and osteoclast lineages.

### *fms* is essential for development of embryonic xanthophores

*fms* mutant larvae lack the yellow color of wild-type larvae at 3 days (Fig. 1A,B), indicating a defect in the xanthophore lineage. This could reflect a failure of xanthophore precursors (xanthoblasts) to differentiate. Alternatively, xanthoblasts could require *fms* for their dispersal from the neural crest, much as melanoblasts or melanocytes require *kit* for their dispersal (Bernex et al., 1996; Parichy et al., 1999). To test these hypotheses, we isolated two markers for the xanthophore lineage: *xanthine dehydrogenase* (*xdh*) and *GTP-cyclohydrolase I* (*gch*). Xdh is required for synthesizing the xanthophore pteridine pigment xanthopterin, and thus should be upregulated in xanthoblasts (Epperlein and Löfberg, 1990; Reaume et al., 1991). Gch converts guanosine triphosphate to tetrahydrobiopterin (BH4), a precursor to pteridine pigments. BH4 also is a co-factor for phenylalanine hydroxylase, which converts phenylalanine to tyrosine (a precursor to melanin), and regulates the activity of tyrosinase, which converts tyrosine to the melanin intermediate, dopa (O'Donnell et al., 1989; Wood et al., 1995; Nagatsu and Ichinose, 1999). Thus, *gch* should be expressed by xanthoblasts, and possibly melanoblasts.

In situ hybridization reveals *xdh*+ cells in neural crest migratory pathways and, at later stages, in regions occupied by xanthophores (Fig. 5A,B), suggesting these cells are xanthoblasts. Additionally, some cells close to the neural crest express both *xdh* and *mitf*, and may represent uncommitted precursors of melanocytes or xanthophores (Fig. 5E). *gch*

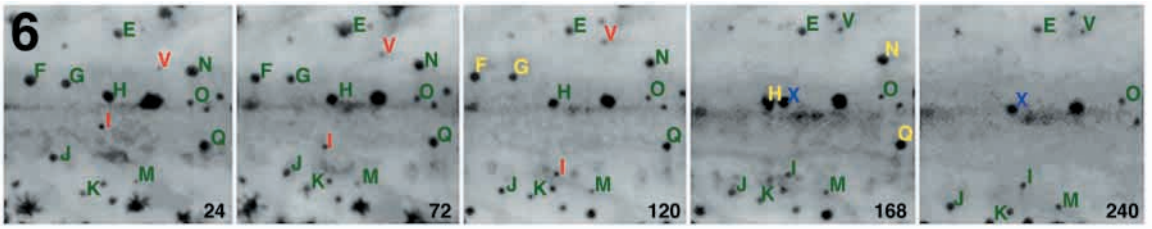


**Fig. 6.** Image analyses reveal *fms* requirement for melanocyte morphogenesis during adult stripe development. Representative images from the flank of a wild-type *D. rerio* larva beginning at 18 days of development. The future interstripe region in the middle of the flank is the image center, and the horizontal line running through each image is the horizontal myoseptum. Anterior is to the left and hours after the start of imaging are in the lower right corner of each frame. Identified melanocytes are indicated with letters immediately to the upper right of each cell; some melanocytes are not lettered here for clarity. Green indicates melanocytes that do not substantially change position between time points. Red indicates migrating melanocytes that change position relative to other cells and landmarks. For example, cell V moves dorsally (compare to cells E and N), whereas cell I moves ventrally (compare to O and Q). Starting and ending positions can be quantified relative to the total height of the flank; e.g., V moves –0.06 dorsally, I moves 0.10 ventrally (see text). Yellow indicates melanocytes that die, as evidenced by their unambiguous disappearance in the next frame. For instance, cells F and G die shortly after 120 hours. Although we cannot formally exclude the possibility that some melanocytes migrated out of the focal plane (e.g., medially within the larva), such peripheral-to-medial movements have not been reported during earlier stages of development (reviewed in: Reedy et al., 1998). In contrast, a few fully differentiated melanocytes appeared during the imaging series, possibly after migrating to the periphery from more medial locations (e.g., cell X; see Milos et al., 1983). Finally, positions and shapes of approx. 1% of cells in both wild-type and *fms* mutant larvae suggested division of fully differentiated melanocytes, consistent with observations in other species (Parichy, 1996a).

expression is similar to *xdh*, and many cells coexpress both *gch* and *xdh* (not shown), though *gch* is also detectable in lightly melanized melanocytes (Fig. 5C,F). Thus, *gch* is likely to be expressed both by xanthoblasts and melanoblasts. Many non-melanized *xdh*+ and *gch*+ cells coexpress *fms* (Fig. 5D,F), consistent with *fms* expression by the xanthophore lineage. To test whether *fms* is required for the migration of xanthoblasts, we examined the distribution of *xdh*+ and *gch*+ cells in *fms* mutant embryos. In contrast to wild type, *fms* mutant *xdh*+ cells were confined to the vicinity of the neural crest, and few unmelanized *gch*+ cells were observed during and after neural crest migration (Fig. 5G-I). These data indicate that *fms* is expressed by the xanthophore lineage, and promotes the dispersal of these cells from the neural crest. Thus, the xanthophore requirement for *fms* parallels the melanocyte requirement for *kit*.

### *fms* promotes patterning of melanocyte death and migration during adult stripe development

*fms* mutant adults lack normal stripes (Fig. 1D). To determine how *fms* promotes stripe development, we compared melanocyte numbers and behaviors ($n$=880 melanocytes total) in image series of wild-type and *fms* mutant larvae during pigment pattern metamorphosis. Because we imaged larvae between 18 and 30 days, these analyses include early larval melanocytes that may have persisted until metamorphosis, adult stripe melanocytes comprising the early (*kit*-dependent) and late (*rose*-dependent) populations, as well as melanocytes that will contribute to adult scales. Xanthophores and iridophores were not visible in these images. At the beginning of the series, wild-type larvae exhibited melanocytes still in the position of early larval stripes, as well as some melanocytes dispersed over the flank (presumptive *kit*-dependent melanocytes). By the end of the image series, an adult pigment pattern had been established, in wild type consisting of two melanocyte stripes (a dorsal stripe at dorsoventral position approx. 0.35, and a ventral stripe at position approx. 0.65; see Materials and Methods), a single, light interstripe region (position approx. 0.5; i.e., the approximate dorsoventral midpoint of the flank), and scale-associated melanocytes in the dorsal region of the flank (position 0-0.5).

Our analyses reveal that melanocyte death in the prospective interstripe region contributes to stripe development in wild-type larvae, whereas a defect in the patterning of melanocyte death is associated with the failure of normal stripe development in *fms* mutant larvae. Previous studies of stripe development in the fin (Goodrich and Nichols, 1931) and early larval melanocytes on the body (Milos et al., 1983) suggested that some melanocytes die if present in prospective interstripe regions (i.e., regions occupied by xanthophores; see Discussion). To test whether melanocyte death has a role in adult body stripe development, we determined the probability that melanocytes followed from day 18 of development (day 1 of imaging) died by day 30 (end of imaging). These melanocytes principally represent cells persisting from the early larval pigment pattern, as well as melanocytes comprising the early appearing *kit*-dependent population of adult stripe melanocytes (and exclude late appearing *rose*-dependent melanocytes that differentiate after approx. 21 days). We could see melanocyte death as an unambiguous disappearance of a melanocyte from one image to the next (Fig. 6). In wild-type larvae, 17±6.8% of these melanocytes ($n$=234) died by day 30. To assess whether melanocytes were more likely to die if located in the prospective interstripe region than stripe regions, we tested for a dependence of melanocyte death on dorsoventral distance from the midpoint of the flank. This analysis revealed that wild-type melanocytes were more likely to die if close to the midpoint (i.e., in the prospective interstripe region). This effect can be visualized as differences in the proportions of melanocytes dying when distance from the midpoint of the flank is divided into discrete regions (Fig. 7A). To assess whether *fms* influences melanocyte death during stripe development, we determined the fate of melanocytes followed from day 18 in *fms* mutant larvae. In *fms* mutants, 26±16.2% of these melanocytes died by day 30 ($n$=207), a significantly greater percentage than in wild type ($\chi^2$=5.88,

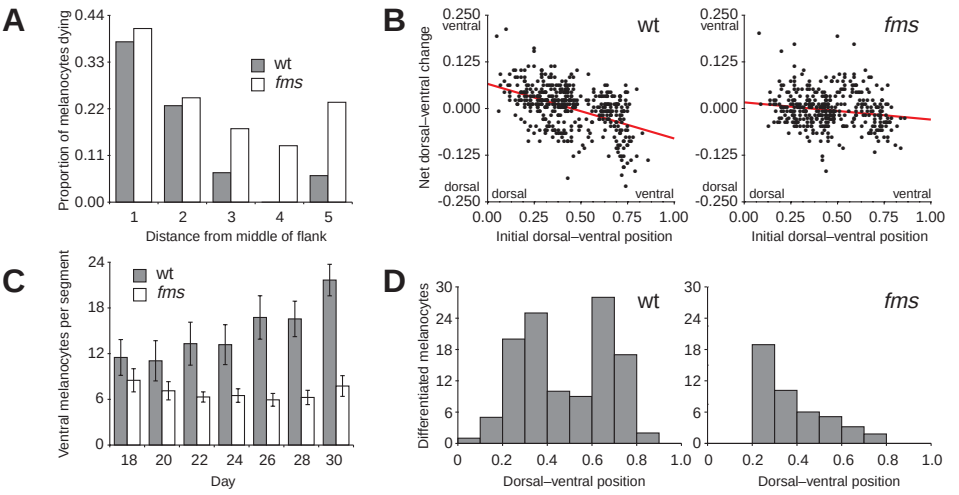


**Fig. 7.** Quantitative analyses of melanocyte death, migration and differentiation reveal differences in pigment pattern development between wild type and *fms* mutants. (A) The proportion of melanocytes dying is shown for regions at different distances from the dorsoventral midpoint of the flank. For clarity of presentation, the flank has been divided into 5 dorsoventral regions: region 1 is the middle of the flank, regions 2-5 are progressively further from the midpoint (in both dorsal and ventral directions). Note the high probability of melanocyte death in region 1 for both wild type and *fms* mutants, and the absence of melanocyte death in region 4 for wild type, but not *fms* mutants. Logistic regression confirms that wild-type melanocytes are more likely to die if close to the midpoint of the flank (logistic regression coefficient –13.8±2.90 (s.e.); $\chi^2$=22.5, d.f.=1, $P$<0.0001), whereas the probability of melanocytes dying in *fms* mutants did not depend on distance from the midpoint (logistic regression coefficient –1.9±1.78 (s.e.); $\chi^2$=1.1, d.f.=1, $P$=0.3), resulting in a significant difference in regression coefficients between genotypes ($\chi^2$=7.9, d.f.=1, $P$<0.005). (B) Patterns of melanocyte movements differ between wild type (left) and *fms* mutants (right). In wild-type larvae, dorsal melanocytes (positions 0.00<0.05) tended to move ventrally (positive net change) and ventral melanocytes (positions 0.5<1.0) tended to move dorsally (negative net change), resulting in a significant relationship between direction of movement and starting position (regression coefficient –0.12±0.009 (s.e.); $t_1$=13.4, $P$<0.0001; $R^2$=0.64; $n$=456 melanocytes). In contrast, this regression is significantly weaker in *fms* mutants ($F_{1,809}$=21.3, $P$<0.0001; regression coefficient –0.05±0.012 (s.e.); $t_1$=3.92, $P$<0.0001; $R^2$=0.26; $n$=390 melanocytes), reflecting a failure of these cells to coalesce into stripes (see text). We can rule out non-isometric growth of the flank as being principally responsible for the melanocyte movements observed here, as *fms* mutants do not exhibit growth defects during these stages of development (data not shown). (C) Numbers of differentiated melanocytes differ between wild type and *fms* mutants (mean total melanocytes±95 C.I. per segment for imaged larvae). Wild-type larvae have progressively more melanocytes per segment than *fms* mutants. (D) The pattern of melanocyte differentiation differs between wild type (left) and *fms* mutants (right). The total numbers of melanocytes that differentiated during the image series at different dorsoventral positions on the flank are shown. More melanocytes differentiated in wild type, and these cells were found in the future stripe regions (approx. 0.35, approx. 0.65). In *fms* mutants, relatively few cells differentiated in future stripe regions, and this is particularly evident ventrally (where cell numbers are not confounded by melanocytes that will localize on scales, not stripes).

d.f.=1, $P$<0.05). Also in contrast to wild type, the likelihood of *fms* mutant melanocytes dying did not depend significantly on distance from the midpoint of the flank (Fig. 7A). Taken together, these data indicate that melanocytes are more likely to die in the prospective interstripe region in wild-type larvae, and a perturbation of Fms signaling results in both an increased total likelihood of melanocyte death and a defect in the patterning of this death.

Image analyses also show that directed melanocyte migration contributes to stripe development in wild-type larvae, and a failure of directed migration is associated with the failure of stripe development in *fms* mutants. In other species, stripes form because initially dispersed melanocytes migrate into prospective stripe regions (Epperlein and Lofberg, 1990; Parichy, 1996a,b). To test whether melanocyte migration is involved in stripe formation in *D. rerio*, and whether migration is perturbed in *fms* mutants, we calculated the relative dorsoventral position of each melanocyte when first identified, and when last observed. For each melanocyte followed more than one day, we then estimated the net change in dorsoventral position by subtracting the starting position from the ending position. These analyses thus include early larval melanocytes, as well as early and late appearing adult melanocytes (analyses limited to melanocytes present at the beginning of imaging yielded qualitatively similar results). In wild-type larvae, dorsal melanocytes tended to move ventrally, whereas ventral melanocytes tended to move dorsally (Fig. 7B). This reflects migration of melanocytes in dorsal and ventral regions of the flank towards the middle of the flank, to form dorsal and ventral stripes, respectively. Although some melanocytes initially in the prospective interstripe region migrated in the reverse direction (e.g., dorsal cells moving further dorsally; Fig. 6), these cells contributed little to the overall pattern of movement (presumably because many melanocytes in the prospective interstripe region died, rather than migrated into stripes). Examination of melanocyte movements in *fms* mutant larvae ($n$=390 melanocytes) revealed that absolute changes in melanocyte position (i.e., independent of direction) did not differ from wild type (least squares means ± s.e. in wild type, *fms* mutants, respectively=0.044±0.004, 0.036±0.005; $F_{1,835}$=0.06, $P$=0.8), indicating that overall melanocyte motility is not impaired in *fms* mutants. Nevertheless, the relationship between direction of movement and position was significantly weaker in *fms* mutant larvae as compared to wild type (Fig. 7B). This difference can be understood as a reduction in organized, directional melanocyte movements when Fms signaling is perturbed.

These data identify roles for *fms* in patterning melanocyte death and migration during stripe development. This could indicate a direct effect on melanocyte behavior, if these cells express *fms*. Or, effects on melanocyte patterning could be indirect, and mediated via interactions between melanocytes and other *fms*-expressing cell types. To distinguish between these possibilities, we examined *fms* expression during adult

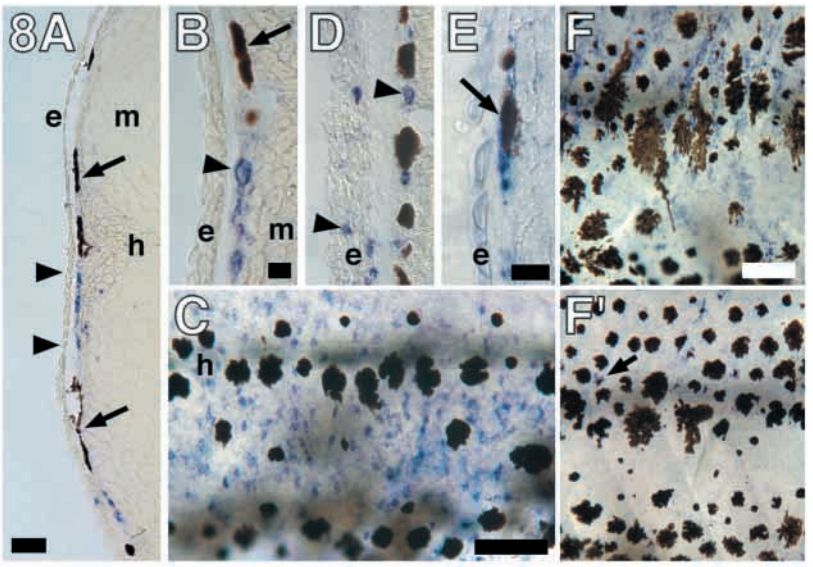


**Fig. 8.** *fms*-dependent adult stripe development. (A-D) *fms* is expressed by cells other than melanocytes during pigment pattern metamorphosis (A,B,D, 8 μm cryosections; C, whole-mount larva). (A) In a cross section through the middle trunk of a 20 day wild-type larva, *fms*+ cells (blue) are present in the prospective interstripe region (bounded by arrowheads). These cells are also abundant dorsally and ventrally (shown in this section) to prospective stripes. Melanocytes are present in prospective dorsal and ventral stripe regions (arrows). e, epidermis; m, myotome; h, horizontal myoseptum. (B) Higher magnification of a 20 day wild-type larva reveals that stripe melanocytes (arrow) do not express *fms*. Arrowhead indicates an unmelanized *fms*+ cell in the prospective interstripe region. (C) *fms*+ cells (blue) are observed widely dispersed over the flank in a 22 day wild-type whole-mount larva. (D) In a 26 day larva, unmelanized *fms*+ cells are more abundant beneath the epidermis and myotome, and also are observed within the epidermis (arrowheads). (E) *kit* expression is detectable in melanocytes during metamorphosis. Shown is a *kit*+ melanocyte (arrow) in a 21 day wild-type larva. (F,F′) *gch* expression differs between wild-type and *fms* mutant larvae in whole-mount 25 day larvae. (F) In wild type, unmelanized *gch*+ cells are abundant over the flank, particularly dorsally and in the prospective interstripe region. (F') In *fms* mutants, however, unmelanized *gch*+ cells are absent, though a few melanin-containing *gch*+ cells persist (e.g., arrow). Scale bars: (A) 50 μm; (B,D) 10 μm; (C) 100 μm; (E) 10 μm; (F,F′) 100 μm.

stripe development. In wild-type larvae, *fms* is expressed by unmelanized cells between the epidermis and myotome (Fig. 8A,C). Although some melanocytes express *kit* during these stages, differentiated melanocytes do not express *fms* (Fig. 8B,D,E). These data suggest that *fms* does not directly promote melanocyte death or migration (although we cannot formally exclude the possibility that differentiated melanocytes express functionally significant levels of *fms* mRNA at a level below the threshold of detection by in situ hybridization). Since xanthophores influence melanophore morphogenesis in other species (Epperlein and Löfberg, 1990; Parichy, 1996b) and xanthophores depend on *fms* for their morphogenesis in *D. rerio* embryos (above), we hypothesized that effects of *fms* on melanocyte death and migration in *D. rerio* might be mediated by interactions between melanocytes and *fms*-dependent xanthophores. To test whether xanthoblasts are present during adult stripe development, we compared the distribution of *gch*+ cells and differentiated xanthophores between wild-type and *fms* mutant larvae and adults (*xdh* staining resulted in excessive background and was not useful during these stages). In wild type, numerous, non-melanized *gch*+ cells are present between the epidermis and the myotome (Fig. 8F), and xanthophores occur outside of prospective stripe regions during metamorphosis, and in interstripe regions in adults (Fig. 2A). In contrast, *fms* mutants lack unmelanized *gch*+ cells (Fig. 8F′), exhibit greatly reduced numbers of xanthophores on the body and in the fins of metamorphosing larvae, and completely lack xanthophores in adults (Fig. 2B). These findings are consistent with a model in which interactions between melanocytes and *fms*-dependent xanthophores contribute to patterning melanocyte death and migration during adult stripe development.

### Late appearing, *kit*-independent stripe melanocytes require *fms* for development

In addition to effects on melanocyte death and migration, the pigment pattern defect in *fms* mutant adults could reflect a difference in melanocyte differentiation. To test this possibility, we first counted melanocytes in imaged larvae between 18 and 30 days. Since many dorsal melanocytes localize on scales rather than in stripes, we limited our analysis to the ventral half of larvae, which lacks prospective scale melanocytes. Fig. 7C shows that ventral melanocytes nearly doubled in number in wild-type larvae, but did not increase in *fms* mutants. To determine whether this difference reflected, in part, a difference in melanocyte differentiation, we assessed the probability that melanocytes identified at 30 days were derived from melanocytes that differentiated between 19 and 30 days (i.e., were not present at the beginning of imaging at 18 days). Newly differentiated melanocytes were readily distinguishable as small, lightly melanized cells in regions not previously occupied by melanocytes. This analysis revealed that over the entire flank in wild-type larvae, 49±6.5% of melanocytes differentiated de novo, whereas in *fms* mutant larvae only 23±12.2% of melanocytes differentiated de novo, resulting in a significant difference between genotypes ($\chi^2$=7.8, d.f.=1, $P$<0.01). Wild-type melanocytes that differentiated during this time were limited principally to dorsal regions (prospective scale and dorsal stripe melanocytes) and ventral regions (prospective ventral stripe melanocytes), and few were found in the middle of the flank (prospective interstripe region; Fig. 7D). In contrast, newly differentiated melanocytes in *fms* mutants were limited principally to dorsal regions (presumably scale melanocytes) and very few differentiated in the region of the ventral stripe. Thus, *fms* is required for the differentiation of normal numbers of melanocytes during adult stripe development. Consistent with this inference, 6 week *fms* mutant juveniles have only approx. 70% as many stripe (i.e., non-scale) melanocytes as wild-type juveniles in dorsal and ventral regions of the flank (Fig. 9E).

Adult melanocyte stripes in *D. rerio* depend on two populations of melanocytes: a *kit*-dependent population arises


**Fig. 9.** Epistasis analysis reveals that *fms* promotes the development of a subpopulation of adult stripe melanocytes. (A,B) *fms* and *rose* promote the development of a common melanocyte population. (A) *rose* mutants have approximately half as many stripe melanocytes as wild type. (B) *fms; rose* double mutants have numerous dermal stripe melanocytes, though unlike *rose* single mutants, these melanocytes remain dispersed over the flank (revealing *fms*-dependency of migration by these residual *kit*-dependent melanocytes; see text). (C,D) *fms* and *kit* are required by different melanocyte populations. (C) A *kit* mutant has about half the wild-type complement of dermal stripe melanocytes. *kit* mutants also lack dermal scale melanocytes normally present over the dorsal flank. With the absence of scale melanocytes, highly abundant xanthophores in dorsal and ventral regions of the flank are visible owing to the orange coloration these cells impart. (D) *fms;kit* double mutant has a much more severe melanocyte deficit than either single mutant, and lacks virtually all stripe and scale melanocytes (as well as xanthophores). *fms;kit* double mutants were not grossly anemic, consistent with previous observations of *D. rerio kit* single mutants (Parichy et al., 1999). (E) Dermal stripe melanocytes (excluding scale melanocytes) in wild type, as well as *fms*, *rose*, *kit*, *fms;rose*, and *fms;kit* mutants. Shown is the mean number of stripe melanocytes/mm±95% confidence intervals ($n$=6 fish per genotype). Horizontal line indicates means that are not significantly different (Tukey-Kramer comparison). Whereas *fms;rose* mutants do not have significantly fewer melanocytes than *rose* single mutants, *fms;kit* double mutants have an additive deficit in melanocyte number, approximately equal to that due to *fms* and *kit* mutations individually.

dispersed over the flank beginning at approx. 14 days, and a *rose*-dependent population arises already in stripes beginning at approx. 21 days (Johnson et al., 1995b). Given the defect in melanocyte differentiation in *fms* mutants, we asked whether *fms* is required by *kit*-dependent melanocytes, *rose*-dependent melanocytes, or both. The increasingly severe deficit in *fms* mutant melanocytes after 22 days (Fig. 7C), and the failure of these cells to differentiate in stripes (Fig. 7D), are consistent with a requirement for *fms* in promoting the appearance of the later, *rose*-dependent melanocytes. To further test this model, we constructed fish doubly mutant with *kit* or *rose*. If *fms* is required by late appearing *rose*-dependent melanocytes, but not early appearing *kit*-dependent melanocytes, two predictions can be made. First, double mutants for *fms* and *rose* should not have a different number of melanocytes than the more severely melanocyte-deficient *rose* single mutant (since the two genes would be acting to affect only one melanocyte population). Second, double mutants for *fms* and *kit* should have an additive deficit in melanocyte number, equal to the reduction attributable to the *fms* mutant alone, plus the reduction due to the *kit* mutant alone (since the two genes would be acting independently to affect two different melanocyte populations). Fig. 9 presents tests of these predictions. We find that *fms; rose* double mutants do not have significantly fewer dermal stripe melanocytes (i.e., non-scale melanocytes) than *rose* single mutants (means=123, 132 melanocytes/mm, respectively; $t_6$=1.36, $P$=0.2; Fig. 9A,B,E), although these cells remain in a dispersed pattern, presumably reflecting the requirement of *fms* for melanocyte migration into stripes (Fig. 7B). In contrast, *fms; kit* double mutants exhibit a dramatic reduction in melanocyte number (mean=36 melanocytes/mm) as compared to either single mutant (*fms* and *kit*, means=181, 96 melanocytes/mm, respectively; Fig. 9C-E). Moreover, this reduction in *fms; kit* double mutants is not significantly different from that predicted (21.7 melanocytes/mm) by additive effects of the two mutations ($t_6$=2.19, $P$=0.1). Together, these data suggest that *fms* is required by late appearing, *rose*-dependent melanocytes, but is not required by early appearing *kit*-dependent melanocytes. Thus, two essentially paralogous genes, *fms* and *kit*, are required by parallel populations of pigment cells: *fms* promotes the development of embryonic and adult xanthophores, as well as late appearing adult melanocytes; whereas *kit* promotes the development of embryonic melanocytes and early appearing adult melanocytes.

## DISCUSSION

We have shown that the *D. rerio* pigment pattern mutant *panther* corresponds to an orthologue of the *kit*-related gene *fms*, and that *fms* is required by embryonic and adult xanthophores, and a subpopulation of adult melanocytes. These results have implications for our understanding of the roles played by receptor tyrosine kinases during development, the cell populations constituting the *D. rerio* adult pigment pattern, and the morphogenetic mechanisms underlying pigment pattern formation.

### Novel roles and phylogenetically conserved roles for *fms* during development

Studies of mouse mutants have identified several genes required for neural crest and pigment cell development, including *kit*, *mitf* and *ednrb* (Bennett, 1993; Shibahara et al., 1998; Reedy et al., 1998). Mutants corresponding to each of these genes now have been identified in *D. rerio*, and all exhibit pigment pattern defects (Parichy et al., 1999; Lister et al., 1999; D. M. P., R. N. Kelsh, S. L. J., unpublished data), revealing a conservation of molecular mechanisms for pigment pattern formation across amniotes and teleosts. In contrast, our demonstration that *panther* is allelic to *fms* is unexpected, as this gene has not previously been implicated in neural crest or pigment cell development. *fms* is the closest known homologue of *kit* and the ligand for the Fms receptor is Colony Stimulating

Factor 1 (CSF1), which has structural similarities to the Kit ligand, Steel Factor (Bazan, 1991). Studies of amniotes, including a CSF1-deficient mouse mutant reveals that Fms is expressed and required by cells of the mononuclear phagocyte system, including macrophages in the reproductive tract and elsewhere, microglia in the central nervous system, and bone-resorbing osteoclasts (Ducy and Karsenty, 1998; Motoyoshi, 1998; Flanagan and Lader, 1998). Although a role for Fms in the development of the amniote neural crest–melanocyte lineage has not been excluded, *Csf1* mutant mice do not exhibit pigmentation defects (Marks and Lane, 1976).

Several studies have indicated that an additional round of genome duplication has occurred in teleosts as compared to amniotes (Postlethwait et al., 1998; Amores et al., 1998). This inference raises the possibility that the gene that we have identified might correspond to a teleost-specific *D. rerio* paralogue of *kit*, rather than a true orthologue of amniote *fms*. Two lines of evidence argue against this notion. First, phylogenetic reconstructions place this gene as more closely related to mammalian *fms* genes than other type III receptor tyrosine kinases, including *D. rerio kit*. Second, our analyses reveal phylogenetically conserved expression in macrophage precursors and osteoclasts. These data strongly support the interpretation that we have isolated a *D. rerio fms* orthologue with a role in pigment pattern development. Nevertheless, we do not exclude the possibility that a second *fms* gene may be present in *D. rerio*, perhaps with more restricted functions than the locus reported here.

### Xanthophore requirement for *fms* parallels melanocyte requirement for *kit*

Pigment patterns in amniotes typically reflect the physiology of epidermal, neural crest-derived melanocytes that contribute melanin to growing hair, feathers or scales. In contrast, pigment patterns in ectothermic vertebrates typically reflect the spatial organization of dermal neural crest-derived melanocytes, xanthophores and iridophores (Quevedo and Holstein, 1998; Bagnara, 1998). Although pigment synthesis genes are presumably expressed differentially across cell types, the extent to which different pigment cell classes share mechanisms of specification and morphogenesis remains unknown. Here, we have shown that *gch+* and *xdh+* presumptive xanthoblasts express *fms* and require this gene for their development, though they do not express or require *kit*. In contrast, *dct+* late-stage melanoblasts express and require *kit*, but not *fms* (Parichy et al., 1999). These findings indicate a common requirement of xanthophores and melanocytes for signaling through type III receptor tyrosine kinases. Indeed, the failure of *xdh+* cells to disperse from the neural crest in *fms* mutant embryos is reminiscent of the failure of melanoblasts to disperse in *kit* mutant embryos (Parichy et al., 1999) and is consistent with shared signal transduction pathways downstream of *fms* and *kit* (Dubreuil et al., 1991). Thus, migration from the neural crest depends, at least in part, on parallel signaling mechanisms in melanocytes and xanthophores.

### *fms* promotes differentiation of a subpopulation of adult melanocytes

A previous study suggested that adult stripes in *D. rerio* arise from temporally and genetically distinct populations of melanocytes (Johnson et al., 1995b). An early developing population initially appears dispersed over the flank and depends on *kit*; a later developing population arises already in the position of adult stripes and depends on *rose*. Support for this model came from the finding that *kit* and *rose* mutations have additive effects, consistent with these genes acting on two different melanocyte populations: whereas *kit* and *rose* single mutants each lack half the normal complement of stripe melanocytes, *kit; rose* double mutants lack virtually all body stripe melanocytes. Two independent lines of analysis support a model in which *fms* promotes the differentiation of *rose*-dependent, but not *kit*-dependent melanocyte precursors. First, image series revealed that *fms* mutants have a severe deficiency in melanocyte differentiation, particularly in prospective stripe regions during late stages of pigment pattern metamorphosis. Second, genetic analysis demonstrated that *fms; rose* double mutants do not have significantly fewer body stripe melanocytes than *rose* single mutants. In contrast, *fms; kit* double mutants have a severe deficiency of stripe melanocytes, approximately that expected from additive effects of the two mutations. Taken together, these results strongly support the inference that early appearing melanocytes depend on *kit*, but not *fms*, whereas later appearing melanocytes depend on *fms* and *rose*, but not *kit*.

At least two models could explain the *fms*-dependence of late appearing melanocytes: signaling through Fms could promote the development of these cells indirectly, via interactions between melanocyte precursors and other *fms*-expressing cell lineages (e.g., see below); or, *fms* could promote the development of melanocyte precursors directly. For example, if *fms* is required for establishing or maintaining a population of precursor cells that is recruited to differentiate at metamorphosis, a disruption of Fms signaling could be manifested late in development as a deficit in the number of melanocytes that differentiate in stripes. Consistent with this idea, we observe *fms* expression in embryonic cells that express both the transcription factor *mitf*, which is expressed by melanoblasts (Opdecamp et al., 1997; Lister et al., 1999), and *gch*, which is expressed both by xanthophore and melanocyte lineages. Existence of pigment stem cells also has been inferred in studies of amniotes (e.g., Grichnik et al., 1996; Kunisada et al., 1998). Thus, we hypothesize that Fms signaling allows the development of a subpopulation of pigment cell precursors – that may or may not be pluripotent – and some of these cells differentiate as melanocytes in the position of stripes during pigment pattern metamorphosis.

### *fms* mutant reveals roles for melanocyte death and migration during adult stripe development

In addition to contributions from localized differentiation and proliferation, adult melanocyte stripes could reflect roles for cell migration and differential cell death. Although several studies have described changes in melanocyte distributions during pigment pattern metamorphosis (Goodrich and Nichols, 1931; Kirschbaum, 1975; Johnson et al., 1995b; McClure, 1999), previous workers have not followed individual cells and thus could not distinguish between roles for different morphogenetic behaviors (e.g., a decrease in cell density could reflect either emigration or death of melanocytes). By observing the behavior of melanocytes in wild-type and *fms* mutants during the larval-to-adult transition, we identified roles

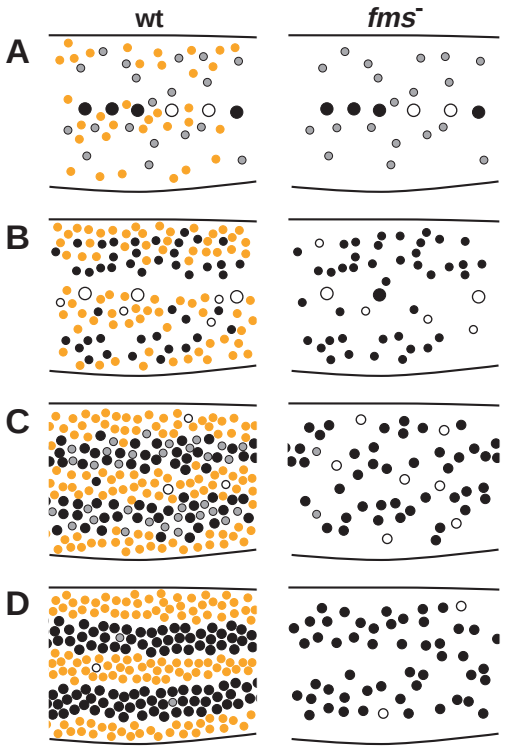


**Fig. 10.** Model for *fms*-dependent adult stripe formation in *D. rerio*. Wild-type larva (left) and a *fms* mutant larva (right) during pigment pattern metamorphosis. Early larval melanocytes are large black cells in the middle of the flank. Newly differentiated and fully differentiated melanocytes are smaller grey and black cells, respectively. For clarity, scale melanocytes are omitted. Dying melanocytes are filled white and xanthophores are orange. (A) At an early stage of pigment pattern metamorphosis in wild type (beginning at approx. 14 days), some early larval melanocytes persist and others die in the middle of the flank. Simultaneously, *kit*-dependent, *fms*- and *rose*-independent early stripe melanocytes begin to differentiate dispersed widely over the flank. A few xanthophores are scattered over the flank, and are somewhat more abundant in the prospective interstripe region. In a *fms* mutant, melanocyte behaviors are the same as wild type, but xanthophores are absent. (B) Subsequently in wild type (approx. 18-21 days), the *kit*-dependent melanocytes increase in number and begin to migrate towards sites of stripe formation, under the influence of *fms*-dependent xanthophores (e.g., Parichy, 1996a). Additional isolated melanocytes in the prospective interstripe region die (compare with Figs 6, 8A). In the *fms* mutant, xanthophores are absent and melanocytes migrate haphazardly; melanocytes die both in the middle of the flank, and regions further dorsally and ventrally. (C) Later in wild-type development (approx. 21-28 days), early *kit*-dependent melanocytes continue to coalesce into stripes. Meanwhile, *kit*-independent but *fms*- and *rose*-dependent melanocytes differentiate already in stripes. In the *fms* mutant, melanocytes have failed to coalesce, owing to the absence of xanthophores, and virtually all *kit*-independent, *fms*-dependent late stripe melanocytes fail to appear. Thus, a threshold density for melanocyte survival is not achieved in some regions, resulting in additional melanocyte death across the entire flank. Moreover, since melanocyte motility is not impaired in *fms* mutants, these cells continue to wander during these stages, and this prevents the formation of stable spots of high melanocyte density. (D) Finally in wild type (>28 days), an initial adult pigment pattern is established comprising two melanocyte stripes with xanthophores outside of stripes. In the *fms* mutant, melanocytes remain irregularly scattered over the flank, and may reach a stage at which they no longer exhibit density-dependent survival (compare with Fig. 2).

both for melanocyte migration and for melanocyte death in pigment pattern metamorphosis. From our analyses of image series and gene expression, we suggest the following model, in which stripe morphogenesis employs both mechanisms (Fig. 10). Initially, melanocytes arise dispersed over the flank. Subsequently, xanthophores arise outside of prospective stripe regions and contribute to organizing melanocytes into stripes in two ways. First, xanthophores stimulate the directed migration of melanocytes into stripes. Second, by organizing melanocytes, xanthophores also increase the local densities of these cells, thereby increasing melanocyte survival (a community effect); melanocytes outside of stripes, in low density regions, lack this community effect on survival and tend to die. In contrast, mutants for *fms* lack xanthophores. Consequently, melanocytes fail to migrate into stripes, resulting in lower melanocyte densities, and thereby lower melanocyte survival throughout the flank.

Roles for *fms* in melanocyte migration and death appear to be indirect, as we did not observe *fms* expression in differentiated melanocytes. A direct role of *fms* in xanthophore development is suggested, however, by the absence in *fms* mutants of both unmelanized *gch*+ presumptive xanthoblasts during metamorphosis and xanthophores in adults. Therefore, the failure of directional melanocyte migration in *fms* mutants, concomitant with the failure of xanthophore development, suggests a role for *fms*-dependent xanthophores in organizing melanocytes into stripes. This inference is consistent with pattern-forming mechanisms in salamander larvae, in which interactions between melanophores and xanthophores stimulate the directed migration of melanophores into horizontal stripes and vertical bars (Epperlein and Löfberg, 1990; Parichy, 1996a,b). Thus, initially dispersed melanocytes in *D. rerio* may be stimulated to coalesce into stripes by ‘population pressure’ (Tucker and Erickson, 1986a,b; Thomas and Yamada, 1992) exerted by *fms*-dependent xanthophores. Indeed, *fms*+ and *gch*+ cells (presumptive xanthoblasts), as well as fully differentiated xanthophores, are abundant both within the prospective interstripe region, and further dorsally and ventrally over the flank, bounding the prospective stripe regions.

Our study also supports a requirement for community effects among melanocytes during normal stripe development. In wild-type larvae (this study) and in the fin (Goodrich et al., 1954; Goodrich and Greene, 1959), xanthophores are abundant in prospective interstripe regions and melanocytes die if present within these regions. Although this might suggest the hypothesis that xanthophores directly promote the death of melanocytes, our findings argue against this possibility as approx. 10% more melanocytes died in xanthophore-deficient *fms* mutants as compared to wild type. Instead, we suggest that increased melanocyte death and the different pattern of this death in *fms* mutants may result from decreased local melanocyte densities owing to a failure of these cells to form stripes. More specifically, analyses of *patchwork* mutant mice imply community effects during melanocyte development, such that a minimum density of these cells is required for their survival (Aubin-Houzelstein et al., 1998). In *fms* mutants, a failure of melanocytes to coalesce and differentiate in stripes would tend to increase the likelihood of melanocyte densities falling below a critical threshold for survival at any given point on the flank. Such a mechanism would explain both the

disorganized pattern of melanocyte death in *fms* mutants, and the death of melanocytes isolated within the prospective interstripe region during normal development. Thus, our findings are consistent with a model in which stripe development in *D. rerio* depends both on melanocyte-xanthophore interactions, and interactions among melanocytes. We emphasize, however, that additional factors are likely to be required for stripe development (e.g., Tucker and Erickson, 1986a; Parichy, 1996a). Indeed, the persistence of poorly formed stripes in the anterior of *fms* mutant adults (Fig. 1D) indicates that stripe development is likely to depend in part on different underlying mechanisms at different axial positions. Finally, the results of this study set the stage for future investigations into the developmental bases for naturally occurring variation in adult pigment patterns and, in this regard, *fms* has recently been implicated as a candidate gene for the evolutionary loss of stripes in the pearl danio, *D. albolineatus* (D. M. P. and S. L. J., unpublished data).

For helpful comments and suggestions on the manuscript, we thank Carol Erickson, Kathy Iovine, Joan Manuel, Mark Reedy and Jim Skeath. Additionally, we are grateful to Matt Clark, Raymond Lee and others of the Washington University-MPIMG Zebrafish EST project (RO1-DK55379) for identification of ESTs used in this study. We thank David Beier for genotyping *fms* on our standard mapping panel. Supported by NIH RO1-GM56988 to S. L. J., NSF-Sloan Postdoctoral Fellowship in Molecular Evolution DBI-9750006 to D. M. P., and NIH 1 P50 DK49216-07 to L. I. Z.; S. L. J. is a PEW Scholar in Biomedical Sciences and L. I. Z. is an Associate Investigator of the Howard Hughes Medical Institute. We thank J. Sheppard and J. Manuel for fish care.

## REFERENCES

**Amores A., Force A., Yan Y.-L., Joly L., Amemiya C., Fritz A., Ho R. K., Langeland J., Prince V., Wang Y.-L., Westefield M., Ekker M. and Posthelthwait J. H.** (1998). Zebrafish *hox* clusters and vertebrate genome evolution. *Science* **282**, 1711-1714.

**Atchley W. R. and Hall B. K.** (1991). A model for development and evolution of complex morphological structures. *Biol. Rev.* **66,** 101-157.

**Aubin-Houzelstein G., Bernex F., Elbaz C. and Panthier J.-J.** (1998). Survival of *patchwork* melanoblasts is dependent upon their number in the hair follicle at the end of embryogenesis. *Dev. Biol.* **198,** 266-276.

**Bagnara J. T.** (1998). Ch. 2. Comparative anatomy and physiology of pigment cells in nonmammalian tissues. In *The Pigmentary System: Physiology and Pathophysiology* (ed. J. J. Nordland, R. E. Boissy, V. J. Hearing, R. A. King and J. P. Ortonne), pp. 9-40. New York, New York: Oxford University Press.

**Bazan J. F.** (1991). Genetic and structural homology of stem cell factor and macrophage colony-stimulating factor. *Cell* **65,** 9-10.

**Bennett D. C.** (1993). Genetics, development, and malignancy of melanocytes. *Int. Rev. Cytol*. **146,** 191-260.

**Bernex F., De Sepulveda P., Kress C., Elbaz C., Delouis C. and Panthier J.-J.** (1996). Spatial and temporal patterns of c-*kit*-expressing cells in $W^{lacZ}$/+ and $W^{lacZ}/W^{lacZ}$ mouse embryos. *Development* **122,** 3023-3033.

**Dubreuil P., Forrester L., Rottapel R., Reedijk M., Fujita J. and Bernstein A.** (1991). The c-*fms* gene complements the mitogenic defect in mast cells derived from mutant *W* mice but not *mi* (*microphthalmia*) mice. *Proc. Natl. Acad. Sci. U.S.A.* **88,** 2341-2345.

**Ducy P. and Karsenty G.** (1998). Genetic control of cell differentiation in the skeleton. *Curr. Op. Cell Biol.* **10,** 614-619.

**Epperlein H.-H. and Löfberg J.** (1990). The development of the larval pigment patterns in *Triturus alpestris* and *Ambystoma mexicanum*. *Adv. Anat. Embryol. Cell Biol*. **118**.

**Erickson C. A. and Perris R.** (1993). The role of cell-cell and cell-matrix interactions in the morphogenesis of the neural crest. *Dev. Biol*. **159,** 60-74.

**Flanagan A. M. and Lader C. S.** (1998). Update on the biologic effects of macrophage colony-stimulating factor. *Curr. Op. Hematol.* **5,** 181-185.

**Gans and Northcutt** (1983). Neural crest and the origin of vertebrates: a new head. *Science* **220**, 268-274.

**Goodrich H. B. and Greene J. M.** (1959). An experimental analysis of the development of a color pattern in the fish *Brachydanio albolineatus* Blyth. *J. Exp. Zool.* **141,** 15-45.

**Goodrich H. B., Marzullo C. M. and Bronson W. R.** (1954). An analysis of the formation of color patterns in two fresh-water fish. *J. Exp. Zool.* **125,** 487-505.

**Goodrich H. B. and Nichols R.** (1931). The development and the regeneration of the color pattern in *Brachydanio rerio*. *J. Morphol.* **52,** 513-523.

**Grichnik J. M., Ali W. N., Burch J. A., Byers J. D., Garcia C. A., Clark R. E. and Shea C. R.** (1996). KIT expression reveals a population of precursor melanocytes in human skin. *J. Invest. Dermatol.* **106,** 967-971.

**Groves A. K. and Bronner-Fraser M.** (1999). Neural crest diversification. *Curr. Topics Dev. Biol.* **43,** 221-258.

**Hall B. K.** (1999). *The Neural Crest in Develoment and Evolution.* New York, NY: Springer-Verlag.

**Hörstadius S.** (1950). *The Neural Crest: Its Properties and Derivatives in Light of Experimental Research.* New York, New York: Oxford University Press.

**Hawkes J. W.** (1974). The structure of fish skin. II. The chromatophore unit. *Cell Tissue Res.* **149,** 159-172.

**Johnson S. L., Africa D., Horne S. and Postlethwait J. H.** (1995a). Half-tetrad analysis in zebrafish: mapping the *ros* mutation and the centromere of linkage group I. *Genetics* **139,** 1727-1735.

**Johnson S. L., Africa D., Walker C. and Weston J. A.** (1995b). Genetic control of adult pigment stripe development in zebrafish. *Dev. Biol.* **167,** 27-33.

**Johnson S. L. and Zon L. I.** (1999). Genetic backgrounds and some standard stocks used in zebrafish developmental biology and genetics. *Methods Cell Biol.* **60,** 357-359.

**Jowett T. and Yan Y.-L.** (1996). Two-color whole-mount *in situ* hybridization. In *A Laboratory Guide to RNA: Isolation, Analysis, and Synthesis* (ed. P. A. Krieg), pp. 381-409. New York, New York: John Wiley and Sons, Inc.

**Kelsh R. N. and Eisen J. S.** (1999). The zebrafish *colourless* gene regulates development of ectomesenchymal neural crest derivatives. *Development* **127,** 515-525.

**Kirschbaum F.** (1975). Untersuchungen über das Farbmuster der Zebrabarbe *Brachydanio rerio* (Cyprinidae, Teleostei). *Wilhelm Roux's Arch.* **177,** 129-152.

**Kunisada T., Yoshida H., Yamazaki H., Miyamoto A., Hemmi H., Nishimura E., Shultz L. D., Nishikawa S.-I. and Hayashi S.-I.** (1998). Transgene expression of steel factor in the basal layer of epidermis promotes survival, proliferation, differentiation and migration of melanocyte precursors. *Development* **125,** 2915-2923.

**Lister J. A., Robertson C. P., Lepage T., Johnson S. L. and Raible D. W.** (1999). *nacre* encodes a zebrafish microphthalmia-related protein that regulates neural crest-derived pigment cell fate. *Development* **126,** 3757-3767.

**MacKenzie M. A. F., Jordan S. A., Budd P. S. and Jackson I. J.** (1997). Activation of the receptor tyrosine kinase Kit is required for the proliferation of melanoblasts in the mouse embryo. *Dev. Biol*. **192,** 99-107.

**Marks S. C. Jr. and Lane P. W.** (1976). *Osteopetrosis*, a new recessive skeletal mutation on chromosome 12 of the mouse. *J. Hered.* **67,** 11-18.

**McClure M.** (1999). Development and evolution of melanophore patterns in fishes of the genus *Danio* (Teleostei: Cyprindae). *J. Morph.* **241,** 83-105.

**Milos N., Dingle A. D. and Milos J. P.** (1983). Dynamics of pigment pattern formation in the zebrafish, *Brachydanio rerio*. III. Effect of anteroposterior location of three-day lateral line melanophores on colonization by the second wave of melanophores. *J. Exp. Zool.* **227,** 81-92.

**Motoyoshi K.** (1998). Biological activities and clinical application of M-CSF. *Int. J. Hematol.* **67,** 109-122.

**Nagatsu T. and Ichinose H.** (1999). Regulation of pteridine-requiring enzymes by the cofactor tetrahydrobiopterin. *Mol. Neurobiol.* **19,** 79-96.

**Nataf V., Lecoin L., Eichmann A. and Le Douarin N. M.** (1996). Endothelin-B receptor is expressed by neural crest cells in the avian embryo. *Proc. Natl. Acad. Sci. U.S.A.* **93,** 9645-9650.

**O'Donnell J. M., McLean J. R. and Reynolds E. R.** (1989). Molecular and developmental genetics of the *Punch* locus, a pterin biosynthesis gene in *Drosophila melanogaster. Dev. Genet.* **10,** 273-286.

**Opdecamp K., Nakayama A., Nguyen M.-T., Hogkinson C. A., Pavan W. J. and Arnheiter H.** (1997). Melanocyte development in vivo and in neural crest cell cultures: crucial dependence on the Mitf basic-helix-loop-helix-zipper transcription factor. *Development* **124,** 2377-2386.

**Parichy D. M.** (1996a). Pigment patterns of larval salamanders

(Ambystomatidae, Salamandridae): the role of the lateral line sensory system and the evolution of pattern-forming mechanisms. *Dev. Biol.* **175,** 265-282.

**Parichy D. M.** (1996b). When neural crest and placodes collide: interactions between melanophores and the lateral lines that generate stripes in the salamander *Ambystoma tigrinum tigrinum* (Ambystomatidae). *Dev. Biol.* **175,** 283-300.

**Parichy D. M., Rawls J. F., Pratt S. J., Whitfield T. T. and Johnson S. L.** (1999). Zebrafish *sparse* corresponds to an orthologue of c-*kit* and is required for the morphogenesis of a subpopulation of melanocytes, but is not essential for hematopoiesis or primordial germ cell development. *Development* **126,** 3425-3436.

**Phillips P. C.** (1999). From complex traits to complex alleles. *Trends Genet.* **15,** 6-8.

**Postlethwait J. H., Yan Y. L., Gates M. A., Horne S., Amores A., Brownlie A., Donovan A., Egan E. S., Force A., Gong Z., Goutel C., Fritz A., Kelsh R., Knapik E., Liao E., Paw B., Ransom D., Singer A., Thomson M., Abduljabbar T. S., Yelick P., Beier D., Joly J. S., Larhammar D., Rosa F., Westerfield M., Zon L. I., Johnson S. L. and Talbot W. S.** (1998). Vertebrate genome evolution and the zebrafish gene map. *Nature Genet.* **18,** 345-349.

**Quevedo W. C. Jr. and Holstein T. J.** (1998). General biology of mammalian pigmentation. In *The Pigmentary System: Physiology and Pathophysiology* (ed. J. J. Nordland, R. E. Boissy, V. J. Hearing, R. A. King and J. P. Ortonne), pp. 43-58. New York, New York: Oxford University Press.

**Reaume A. G., Knect D. A. and Chovnick A.** (1991). The *rosy* locus in *Drosophila melanogaster*: xanthine dehydrogenase and eye pigments. *Genetics* **129,** 1099-1109.

**Reedy M. V., Parichy D. M., Erickson C. A., Mason K. A. and Frost-Mason S. K.** (1998). Ch. 5. The regulation of melanoblast migration and differentiation. In *The Pigmentary System: Physiology and Pathophysiology* (ed. J. J. Nordland, R. E. Boissy, V. J. Hearing, R. A. King and J. P. Ortonne), pp. 75-95. New York, New York: Oxford University Press.

**Reith A. D., Ellis C., Lyman S. D., Anderson D. M., Williams D. E., Bernstein A. and Pawson T.** (1991). Signal transduction by normal isoforms and *W* mutant variants of the Kit receptor tyrosine kinase. *EMBO J.* **10,** 2451-2459.

**Reith A. D., Ellis C., Maroc N., Pawson T., Bernstein A. and Dubreuil P.** (1993). 'W' mutant forms of the Fms receptor tyrosine kinase act in a dominant manner to suppress CSF-1 dependent cellular transformation. *Oncogene* **8,** 45-53.

**Reith A. D., Rottapel R., Giddens E., Brady C., Forrester L. and Bernstein A.** (1990). *W* mutant mice with mild or severe developmental defects contain distinct point mutations in the kinase domain of the c-*kit* receptor. *Genes Dev.* **4,** 390-400.

**Roberts W. M., Look A. T., Roussel M. F. and Sherr C. J.** (1988). Tandem linkage of human CSF-1 receptor (c-*fms*) and PDGF receptor genes. *Cell* **55,** 655-661.

**Roodman G. D.** (1996). Advances in bone biology: the osteoclast. *Endocrin. Rev.* **17,** 308-332.

**Rousset D., Agnès F., Lachaume P., André C. and Galibert F.** (1995). Molecular evolution of the genes encoding receptor tyrosine kinase with immunoglobulinlike domains. *J. Mol. Evol.* **41,** 421-429.

**Shanubhogue A. and Gore A. P.** (1987). Using logistic regression in ecology. *Current Science* **56,** 933-935.

**Shibahara S., Yasumoto K.-I. and Takahashi K.** (1998). Genetic regulation of the pigment cell. In *The Pigmentary System: Physiology and Pathophysiology* (ed. J. J. Nordland, R. E. Boissy, V. J. Hearing, R. A. King and J. P. Ortonne), pp. 251-273. New York, New York: Oxford University Press.

**Shin M. K., Levorse J. M., Ingram R. S. and Tilghman S. M.** (1999). The temporal requirement for endothelin receptor-B signalling during neural crest development. *Nature* **402,** 496-501.

**Sokal R. R. and Rohlf F. J.** (1981). *Biometry.* New York, New York: W. H. Freeman and Company.

**Swofford, D. L.** (1999) PAUP*. Phylogenetic Analysis Using Parsimony (*and Other Methods). Version 4. Sunderland, Massachusettes: Sinauer Associates.

**Tata J. R.** (1993). Gene expression during metamorphosis: an ideal model for post-embryonic development. *BioEssays* **15,** 239-248.

**Thomas L. A. and Yamada K. M.** (1992). Contact stimulation of cell migration. *J. Cell Sci.* **103,** 1211-1214.

**Tucker R. P. and Erickson C. A.** (1986a). The control of pigment cell pattern formation in the California newt, *Taricha torosa*. *J. Embryol. Exp. Morphol.* **97,** 141-168.

**Tucker R. P. and Erickson C. A.** (1986b). Pigment cell pattern formation in *Taricha torosa:* the role of the extracellular matrix in controlling pigment cell migration and differentiation. *Dev. Biol.* **118,** 268-285.

**Wehrle-Haller B. and Weston J. A.** (1995). Soluble and cell-bound forms of steel factor activity play distinct roles in melanocyte precursor dispersal and survival on the lateral neural crest migration pathway. *Development* **121,** 731-742.

**Westerfield M.** (1993). *The Zebrafish Book.* Eugene, Oregon: University of Oregon.

**Wood J. M., Schallreuter-Wood K. U., Lindsey N. J. and Gardner M. L.** (1995). A specific tetrahydrobiopterin binding domain on tyrosinase controls melanogenesis. *Biochem. Biophys. Res. Comm.* **206,** 480-485.

**Yarden Y. and Ullrich A.** (1988). Growth factor receptor tyrosine kinases. *Ann. Rev. Biochem.* **57**, 443-478.